Polymer xxx (2018) xxx-xxx

Contents lists available at ScienceDirect

Polymer

journal homepage: www.elsevier.com

Preparation and characterization of dual-curable off-stoichiometric amine-epoxy thermosets with latent reactivity

Osman Konuray[a], Nuria Areny[a], José M. Morancho[a], Xavier Fernández-Francos[a], Àngels Serra[b], Xavier Ramis[a, *]

[a] Thermodynamics Laboratory, ETSEIB Universitat Politècnica de Catalunya, Av. Diagonal 647, 08028, Barcelona, Spain
[b] Department of Analytical and Organic Chemistry, Universitat Rovira i Virgili, C/ Marcel lí Domingo s/n, Edifici N4, 43007, Tarragona, Spain

ARTICLE INFO

Article history:
Received 27 February 2018
Received in revised form 5 April 2018
Accepted 11 May 2018
Available online xxx

Keywords:
Epoxy
Diamine
Dual-curing
Latent base
Thermosets

ABSTRACT

A new family of dual-curable poly(hydroxyamine)-poly(ether) thermosets based on off-stoichiometric amine-epoxy formulations has been prepared and characterized. The first curing stage was a self-limiting click epoxy-amine polycondensation with an excess of epoxides and the second stage was an anionic homopolymerization of the unreacted epoxy groups, initiated by a latent base. The curing process was sequential with storage stable intermediate materials. The latency of these partially-cured intermediate materials was established not only by a thermally activated base generator, but also by the vitrification of the formulations. The intermediate and final materials exhibit a wide range of properties depending on the relative contribution of both curing stages. Intermediate materials can either be shape conformable solids, or liquids that are applicable as adhesives. Fully cured materials exhibit shape-memory effect.

1. Introduction

Dual-curing is a methodology in which two different polymerization processes take place sequentially or simultaneously during curing of thermosetting resins. Sequential dual curing presents significant advantages in terms of control of the process and the formed network. Materials can be partially cured before their storage, processing or assembly. Final properties can be achieved whenever desired by using heat or UV light in order to cure the materials fully. Recently, sequential curing is being used with different chemistries for various high added-value applications where custom-tailored materials, processing flexibility and intermediate latency and conformability are required [1,2].

The most prominent applications of dual-curing processing are shape memory polymers [3–6], dry adhesive bonding [7], optical materials [8,9], photolithography [3,10], structured surface topologies [11–14], and holographic materials [15,16].

Among the various strategies employed in dual-curing systems, many recent papers investigate the use of off-stoichiometric formulations [8,17–22]. In these systems, the first curing stage is a self-limiting step-growth reaction with an excess of one monomer that can react during the second stage via a photoinitiated or thermally initiated chain-growth polymerization. In general, all systems prepared with this methodology reach practically complete conversions and the resulting materials exhibit a wide array of properties. Usually, when the second step is triggered by means of UV light, the intermediate materials are easily handled, show high latency in reactivity, are conformable (above the gel point), or show adhesive properties (below the gel point). On the other hand, if the second stage is thermally triggered, the dual curing may cease to be sequential with unstable intermediate materials.

A new dual-curing system based on off-stoichiometric thiol-epoxy formulations was recently developed in order to increase the glass transition temperature and rigidity of base-catalyzed click thiol-epoxy thermosets [23]. Sequential two-step process could be achieved using a tertiary amine catalyst thanks to the selectivity and faster kinetics of thiol-epoxy polycondensation over epoxy homopolymerization. Materials were stable in the intermediate state, after thiol-epoxy reaction, allowing safe storage and manipulation until the second curing stage was initiated. In the same way, the use of an epoxy excess in epoxy-amine or epoxy-anhydride formulations was demonstrated. The epoxy excess helps further crosslinking by epoxy homopolymerization at higher temperatures, but the two curing stages overlapped partially or totally [24–26]. Morancho et al. described the dual curing of off-stoichiometric diethylenetriamine-diglycidyl ether of bisphenol A using 2-methylimidazole as anionic initiator for high temperature homopolymerization of the epoxy excess [26]. After the first curing stage, formulations showed latency and could be safely stored below their glass transition temperatures. However a certain part of the epoxide excess reacted during epoxy-amine condensation (first stage of curing).

Controlled curing sequences can be achieved by using latent catalysts that are activated upon irradiation or temperature. Since 1987, when the first photogenerator was introduced, many new photobases were described [27–29]. Recently tetraphenylborate salts of different bases [30,31] were presented as novel photolatent catalysts of differ-

* Corresponding author.
Email address: ramis@mmt.upc.edu (X. Ramis)

https://doi.org/10.1016/j.polymer.2018.05.040
0032-3861/

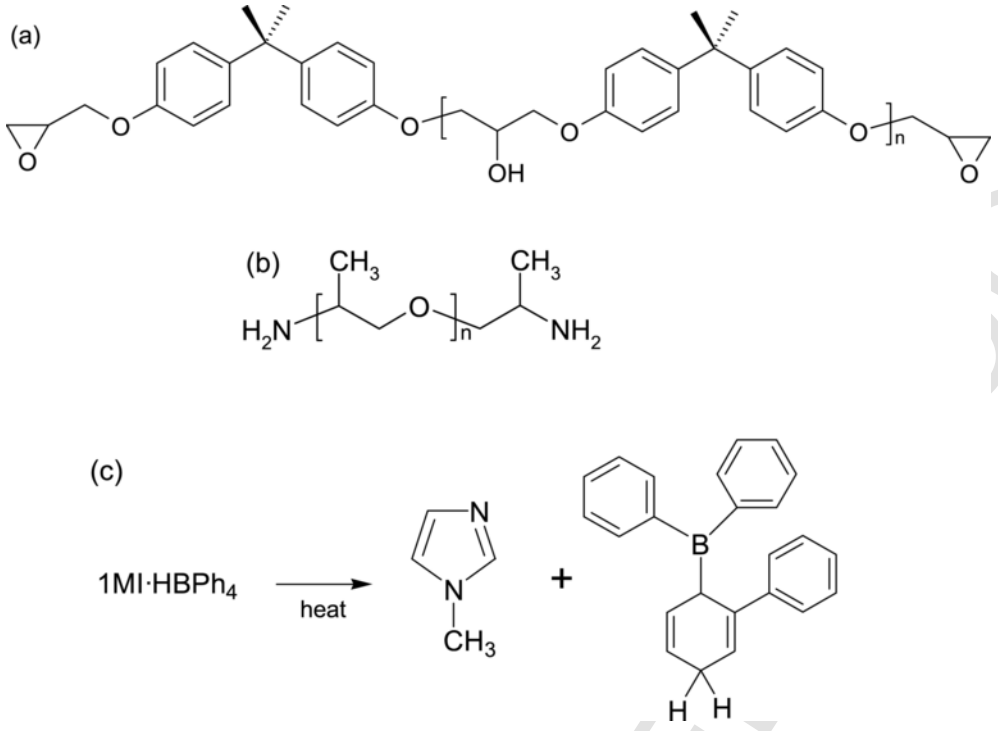

Scheme 1. Molecular structures of the chemicals used: (a) DGEBA, (b) Jeffamine and (c) 1MI·$HBPh_4$ and the compounds formed in its thermal decomposition.

ent reactions such as Michael additions [32], thiol-isocyanate reaction and thiol-epoxy reaction [32–35] and were used in several dual-curable systems (e.g. thiol-acrylate-epoxy or thiol-acetoacetate-acrylate) [36,37]. Kim and Chun cured a naphthalene-based epoxy resin using 2-ethyl-4-methyl imidazolium tetraphenyl borate as latent catalyst [38]. Imidazolium ionic liquids containing alkyl chains and dicyanamide, tetrafluoroborate, or chloride anions were as latent hardeners of bisphenol A-based epoxy resin by Maka et al. [39]. Konuray *el al.* [33] have described the use of 1,5,7-triazabicyclo[4.4.0]dec-5-ene tetraphenylborate as photobase generator in epoxy-thiol curing and they demonstrated that the photobase can be activated either thermally or by UV light. Whereas UV activation could take place at room temperature, thermal activation needs temperatures higher than 100 °C. These results suggest the potential of this type of latent bases in dual curing systems. In these systems, the uncatalyzed first curing stage would take place at low temperatures. This would be followed by an intermediate storage period during which the materials would have reactive stability. Finally, the second stage can be activated in a controlled manner at higher temperatures.

Taking all of this into account, in the present publication we report the preparation and characterization of a new family of thermosets based on off-stoichiometric amine-epoxy formulations. A new, thermally activated base generator 1-methylimidazolium tetraphenylborate was prepared and used. The first stage of curing (stage 1) was an autocatalyzed epoxy-amine polycondensation at a relatively low temperature and the second stage (stage 2) was epoxy anionic homopolymerization of the excess of epoxy groups at a higher temperature. Stage 2 was catalyzed by 1-methylimidazole released by the base generator. The objective of this work was three-fold: a) development of a new dual-curing concept based on the combination of two thermal curing processes at different temperatures for flexible processing and tailoring of intermediate and final materials, b) exploration of the use of tetraphenylborate salts as thermal base generators and c) enhancement of the thermomechanical properties of click epoxy-amine thermosets.

The kinetics of both curing stages, the conversion achieved and the latency after stage 1 were studied by calorimetry and FTIR spectroscopy. Gelation during epoxy-amine condensation was determined by thermomechanical analysis. The materials obtained were characterized by calorimetric, dynamomechanical and thermogravimetric analyses. All materials were stable after stage 1 and they exhibited a wide array of properties depending on the relative contribution of both curing stages. Gelled intermediate materials were highly conformable and shape memory behaviour was observed in complete cured materials.

2. Materials and methods

2.1. Materials

Diglycidyl ether of bisphenol A (DGEBA, M_w = 374 g/mol or M_w = 187 g/ee, Epikote™) (DG hereafter) was kindly supplied by Hexion speciality Chemical B.V. and dried in vacuum before use. Poly(propylene glycol) bis(2-aminopropyl ether) (Jeffamine, M_w = 400 g/mol) (JEF hereafter), 1-methylimidazole (1MI) and sodium tetraphenylborate ($NaBPh_4$) were supplied by Sigma-Aldrich and used as received. Methanol (MeOH) and chloroform ($CHCl_3$) were supplied by VWR and were used as received (see Scheme 1).

1M1·$HBPh_4$ (BG hereafter) was prepared using the procedure outlined in Ref. [31]. Firstly, 1MI was solubilized in H_2O slightly acidified with 36% HCl solution (10 mmol 1MI in 2,6 mL H_2O and 1 mL HCl). $NaBPh_4$ was also solubilized in H_2O (11 mmol in 10 mL H_2O) and stirred until homogeneous. The two solutions were mixed and the stirring maintained until the white salt formed as precipitate. The salt was filtered, washed thoroughly with distilled water and MeOH, recrystallized from a 4:1 mixture of MeOH and $CHCl_3$, filtered and dried under mild temperature and vacuum. To analyze its purity, its melting point was measured in a DSC thermal scan and was

found to be similar to what is reported by other equivalent salts [30,33].

2.2. Sample preparation

Samples were prepared in 5 mL vials in 1–2 gr batches using the following procedure: BG was weighed and added to DG and was kept under agitation at 90 °C for 15 min at complete solubilization. The mixture was left to cool down to room temperature after which the required amount of JEF was added, quickly stirred and immediately sent to analysis or sample preparation. For comparison purposes, some formulations with 1MI and without initiator were also prepared. In these cases, all the liquid components were mixed directly at room temperature. We coded our epoxy-mixtures as DGJEF_x_BG4, where x indicates the fraction of epoxy groups that undergo homopolymerization at stage 2, and 4 is the BG content in weight percentage (%) with respect to the total mass of mixture. As an example, DGJEF_0.5_BG4 is a formulation in which one half of epoxy equivalents react with amine hydrogens and the other half homopolymerizes at stage 2, and contains 4 (%, w/w) of BG. Neat formulations were coded as DGJEF (stoichiometric epoxy-amine formulation without initiator) and DG_BG4 (pristine DG with 4 (%, w/w) of BG). For comparison purposes, in our preliminary study we also prepare the following formulations: DG_1MI2 (pristine DG with a 2 (%, w/w) of 1MI), DGJEF_0.5_1MI2 and DGJEF_0.5 (formulation without initiator). Table 1 shows the composition of the different formulations.

Intermediate and fully cured samples for dynamic mechanical analysis and thermal analysis assays were prepared in a polypropylene mould with dimensions about $1 \times 13 \times 20\,mm^3$. The liquid formulations were poured into the mould and kept in an oven at 90 °C for 240 min to carry out the epoxy-amine condensation. Some of these samples were subsequently cured at 180 °C for 240 min to carry out the anionic epoxy homopolymerization. By means of a dynamic postcuring in a DSC it was checked that the curing was complete at the end of both curing stages. Intermediate formulations showed a residual heat proportional to the epoxy excess and final materials did not show any residual heat.

Table 1
Notation and composition of the formulations studied in this work. The bottom of the table shows the formulations studied only in the preliminary study.

Formulation	r[a]	eq. base/ee	$W_{stage\ 1}/W_{tot}$[d] (%)	$W_{stage\ 2}/W_{tot}$[d] (%)	W_{base}/W_{tot}[d] (%)
DGJEF	1	–	100	–	–
DGJEF_0.25_BG4	1.33	0.100[b]	79	17	4
DGJEF_0.5_BG4	2	0.047[b]	58	38	4
DGJEF_0.75_BG4	4	0.028[b]	33	63	4
DGJEF_0.9_BG4	10	0.022[b]	14	82	4
DG_BG4	–	0.019[c]	–	96	4
DGJEF_0.5_1MI2	2	0.057	59	39	2
DGJEF_0.5	2	–	60	40	
DG_1MI2	–	0.046	–	98	2

[a] Ratio between epoxy groups and reactive amine hydrogens.
[b] Equivalents of 1MI/Equivalents of epoxy excess.
[c] Equivalents of 1MI/Equivalents of epoxy groups.
[d] Weight fractions (%) of stage 1, stage 2 and base respect to the total weight.

2.3. Fourier infrared spectroscopy (FTIR)

In order to monitor the dual-curing process and to verify the degree of cure, a Bruker Vertex 70 FTIR spectrometer equipped with an attenuated total reflection (ATR) accessory (GoldenGate™, Specac Ltd.) was used. Spectra were collected in absorbance mode with a resolution of $4\,cm^{-1}$ in the wavelength range from 4000 to $600\,cm^{-1}$ averaging 20 scans for each spectrum. The spectra were corrected taken into account the dependence of the penetration on the wavelength and normalized using the area of the phenyl group at $1509\,cm^{-1}$. The disappearance of the absorbance peak at $915\,cm^{-1}$ (epoxy bending) [40] was used to monitor the epoxy conversion. According to DSC results, it was observed in all formulations that the conversion was complete at the end of both curing stages. As an example, Fig. 1 shows some spectra collected during reaction at 90 °C of formulation DGJEF (only stage 1) and the calculated conversion. It can be observed the complete disappearance of the epoxy band at $915\,cm^{-1}$.

2.4. Gelation

A Mettler thermo-mechanical analyzer SDTA840 was used to determine the gel point during epoxy-amine polycondensation (stage 1). A silanized glass fiber disc about 5 mm in diameter was impregnated with the liquid (uncured) formulation and sandwiched between two

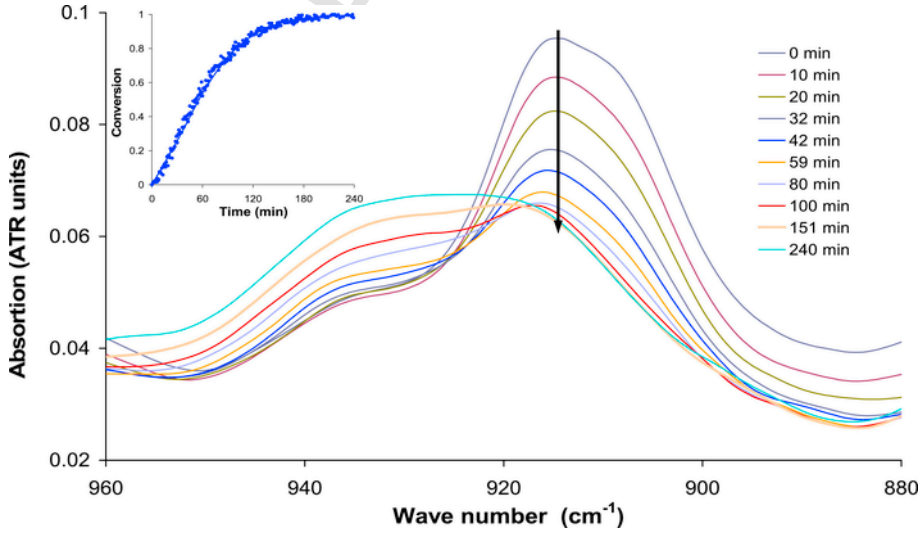

Fig. 1. Evolution of FTIR spectra at 90 °C for DGJEF monitored during epoxy-amine polycondensation for 240 min. Inset shows epoxy conversion versus time for the same formulation.

aluminium discs. The sample was placed at 90 °C for 240 min and subjected to an oscillatory force from 0.005 to 0.1 N with an oscillation frequency of 0.083 Hz. The gel time, t_{gel}, was taken as the onset in the decrease of the oscillation amplitude measured by the probe. The conversion of epoxy groups at the gel point, α_{gel}, was determined as the conversion reached in the DSC at the gel time.

The theoretical conversion of epoxy groups at the gel point, α_{gel}, during epoxy-amine condensation (stage 1) was calculated assuming ideal random step-wise reaction, using the well-known Flory-Stockmayer equation [41,42]:

$$\alpha_{gel}^{theor} = \frac{1}{\sqrt{r(f-1)(g-1)}}$$

where r is the epoxy/hydrogen amine equivalent ratio, $f=2$ the epoxy monomer functionality and $g=4$ the amine functionality.

2.5. Differential scanning calorimetry (DSC)

Calorimetric analyses were carried out on a Mettler DSC822e (dynamic experiments) or on a Mettler DSC821 thermal analyzer (isothermal experiments). Both calorimeters were calibrated using an indium (heat flow calibration and temperature calibration) and zinc (temperature calibration) standards. DSC was either used to monitor reactions heats and residual reaction heats or to determine glass transition temperatures (T_g). Samples of approximately 10 mg were placed in aluminium pans with pierced lids and analyzed under N_2 atmosphere. Dynamic curings, postcurings and T_g determinations were performed by choosing a temperature ramp of 10 °C/min from −100 °C to 300 °C.

Tg's were determined as the temperature of the half-way point of the jump in the heat capacity (ΔC_p) when the material changed from glassy to the rubbery state under N_2 atmosphere and the error was estimated as ± 1 °C. ΔC_p's of intermediate and final materials were also measured. The T_g of samples in the intermediate state was analyzed after isothermal cure for 240 min at 90 °C (stage 1) and that of the fully cured material was determined after stage 1 and subsequently isothermal cure for 240 min at 180 °C (stage 2). *Tg*'s of the intermediate and final materials were also estimated using the copolymer rule given by Fox equation [43], the weight compositions and the experimental T_g of both epoxy-amine network and epoxy homopolymer network in their cured or uncured states, depending on the curing stage analyzed.

Calorimetric degree of conversion was determined as the quotient between the reaction heat released up to a temperature and the total reaction heat.

2.6. Dynamic mechanical analysis (DMA)

Fully-cured materials were analyzed using a TA Instruments DMA Q800 device. Prismatic rectangular samples (about $1 \times 13 \times 20\,mm^3$) were analyzed by DMA using a single cantilever clamp at a frequency of 1 Hz and 0.05% strain at 3 °C/min from −50 °C up to a temperature sufficiently high for complete network relaxation. The peak temperatures of tanδ curves were taken as α-relaxation temperatures, related with the glass transition temperatures.

2.7. Thermogravimetric analysis (TGA)

Thermogravimetric analysis was carried out with a Mettler TGA/SDTA 851e/LF/1100 thermobalance. Samples, obtained by dual curing, with an approximate mass of 10 mg were degraded between 30 and 800 °C at a heating rate of 10 °C/min in N_2 atmosphere (50 cm^3/min measured in normal conditions).

2.8. Latency test

The latency tests were performed for all formulations. After stage 1 (240 min at 90 °C), samples were stored in a thermostatic oil bath at controlled temperatures of 30 °C. T_g's and residual heats of intermediate materials at different times of storage were measured by DSC. Intermediate materials will be reactively stable as long as their T_g and residual heats stay constant (and equal to the reaction heat of Stage 2).

3. Results and discussion

3.1. Preliminary results

First of all, we investigated the possibility of using 1MI as initiator of the epoxy homopolymerization in order to obtain a sequential dual curable system. DGJEF, DG_1MI2 and DGJEF_0.5_1MI2 formulations were dynamically cured at 10 °C/min (see Fig. 2a). The reaction heats of all three systems were close to 100 kJ/ee, a value simi-

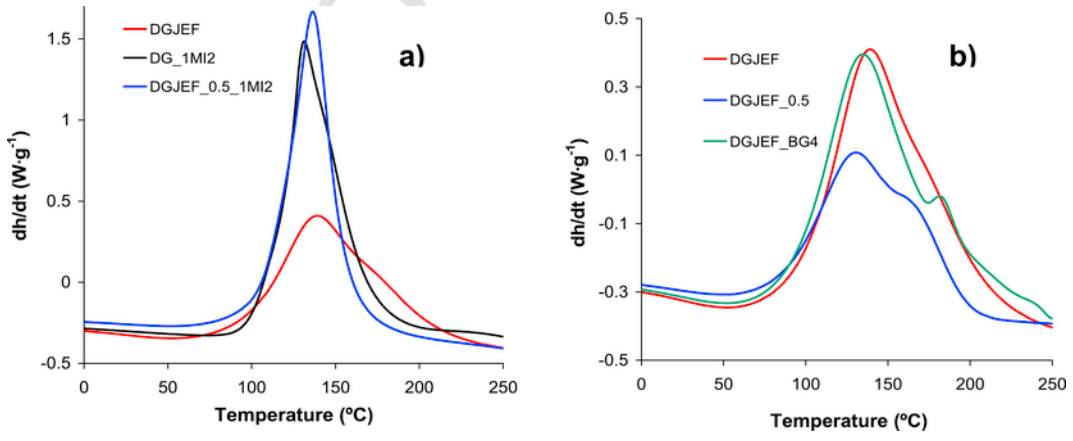

Fig. 2. DSC thermograms corresponding to the dynamic curing at 10 °C/min of **(a)** DGJEF, DGJEF_0.5_1MI2 and DG_1MI2 (effect of 1MI) and **(b)** DGJEF, DGJEF_0.5 and DGJEF_0.5_BG4 (effect of BG and epoxy excess on epoxy-amine condensation).

lar to the one reported for the polymerization of similar epoxy systems [44,45]. This indicates that epoxides reacted almost completely. Fig. 2a shows that 1MI accelerated the epoxy-amine polycondensation but a sequentiality in curing could not be achieved, since DG homopolymerizes in the presence of 1MI in the same temperature range with the epoxy-amine reaction. This is caused in part by the lower reactivity of JEF in comparison with other aliphatic amines such as diethylene triamine or hyperbranched poly(ethyleneimine)s [46]. Moreover, epoxy homopolymerization takes places faster than epoxy-amine polycondensation, contrary to what is desired. Consequently 1MI was ruled out and the latent base (BG) was used for dual curing.

Secondly, we studied the influence of BG and the excess of epoxy groups on epoxy-amine polycondensation kinetics (stage 1). It can be observed (Fig. 2b) that BG and epoxy excess barely modified the curing profile of DGJEF and only a shoulder, associated to the BG decomposition/activation, appeared at 180 °C. In the absence of added catalyst, DGJEF_0.5 formulation did not experience further curing after completion of the epoxy-amine polycondensation.

Thirdly, stage 2 and the dual curing were investigated for the DGJEF_0.5 formulation. Fig. 3 shows how DGJEF_0.5_BG4 exhibits a sequential dual-curing profile. The three peaks are associated, in increasing temperature, to epoxy-amine condensation, BG activation, and homopolymerization of epoxy excess. These processes can be easily identified by comparing DGJEF_0.5_BG4 formulation with DGJEF_0.5 (neat stage 1) and DGJEF_0.5_BG4 (neat stage 2). This last formulation was previously cured 240 min at 90 °C (safely below stage 2 temperature) in order to complete the epoxy-amine condensation. Stage 1, stage 2 and the dual process exhibit reaction heats of 50, 52 and 101 kJ/ee, respectively. This indicates that all epoxy groups have reacted completely. The curing of DG_BG4 formulation was also studied (see *inset* Fig. 3). Compared to this formulation, it can be observed that epoxy homopolymerization takes places at lower temperatures in the presence of JEF (observe the thermogram for DGJEF_0.5_BG4, dual). It can be hypothesized that hydroxyls and tertiary amines formed during epoxy-amine reaction can accelerate the activation of BG and the consequent homopolymerization. It is known that the initiation of epoxy homopolymerization with tertiary amines is favoured by the presence of proton donors. Rozenberg suggested that the use of amines together with tertiary amines in epoxy formulations could have a synergistic effect in terms of reaction kinetics because of the generation of hydroxyl groups by the epoxy-amine condensation [25,47,48].

Finally we studied the isothermal sequential curing of DGJEF_0.5_BG4 formulation. According to the DSC results given in Fig. 3, curing times and temperatures were selected sufficiently low to ensure: a) that the epoxy excess does not react during stage 1, b) the stability of intermediate material and c) that thermal degradation does not take place during stage 2. Samples were cured at different curing times and temperatures (stage 1 between 70 and 100 °C and stage 2 between 140 and 180 °C), in order to achieve complete conversion of epoxy groups at the end of both curing stages. Fig. 4 shows, the conversions achieved in DSC during the two consecutive curing stages: 240 min at 90 °C followed by 240 min at 180 °C. It can be observed that both curing stages reach completion, indicated by a fractional conversion of 0.5 and 1 at the end of stage 1 and stage 2, respectively. This result was confirmed by FTIR and also by a subsequent DSC scan during which no residual heat was detected up to 300 °C. Although latency was tested systematically at a later phase in the study, it was already evident that the intermediate materials can be safely stored, since stage 2 can only be activated by heating to a significantly higher temperature. Similar results to those shown in Fig. 4 were obtained for all formulations. Taking into account all these preliminary results, a new dual-curable family of poly(hydroxyamine)-poly(ether) thermosets with a broad range of properties after both stages of curing (see Table 1) were prepared. The same curing schedule as in Fig. 4 was used to prepare the thermosets.

3.2. Dual-curing and thermal properties of epoxy-amine mixtures

As explained in the experimental section, the new epoxy-amine materials were isothermally dual-cured in the DSC. Samples for DMA were cured in an oven. Table 2 shows some characteristic parameters of the curing and the glass transition temperatures and heat capacity changes for uncured, intermediate and fully cured materials. In general, it can be observed that parameters change as a function of composition. The similarity between the total reaction heats (values close to 100 kJ/ee) and those reported for similar epoxy systems indicates that epoxides reacted almost completely [44,45]. Moreover, the reaction heats associated with stages 1 and 2 are proportional to the

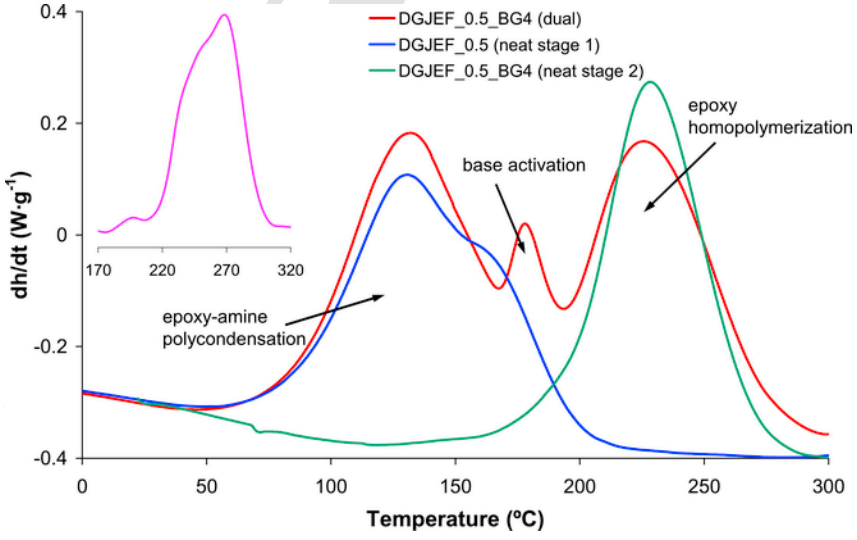

Fig. 3. DSC thermograms corresponding to the dynamic curing at 10 °C/min of DGJEF_0.5 (neat stage 1), DGJEF_0.5_BG4 (dual) and DGJEF_0.5_BG4 (neat stage 2). Inset shows the dynamic curing of DG_BG4 formulation.

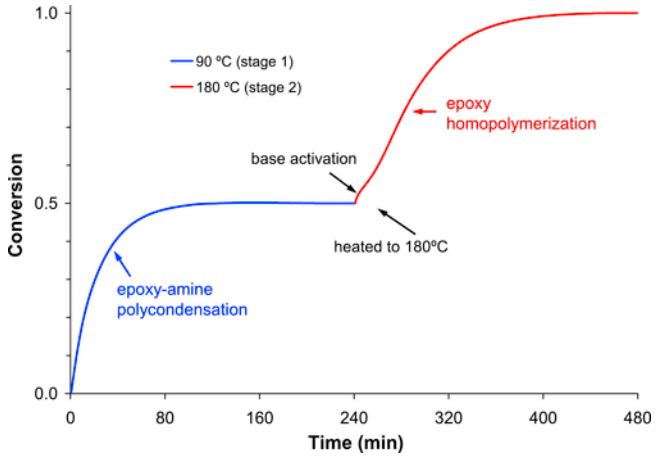

Fig. 4. DSC epoxy conversion during isothermal curing at 90 °C (Stage 1) and later at 180 °C (Stage 2) DGJEF_0.5_BG4.

amount of total epoxy groups present in the formulations. This result demonstrates the high efficiency of click epoxy-condensation and the ability of the BG to promote the epoxy homopolymerization.

Unreacted materials have decreasing T_g and increasing ΔC_p with increasing JEF content, due to the high flexibility of this amine monomer. It can be observed that the T_g after epoxy-amine polycondensation decreases with increasing DG content, due to the plasticizing effect of the DG excess. Accordingly, ΔC_p increases with increasing DG content. For all formulations, a significant increase in T_g takes place during stage 2 due to the homopolymerization of the excess of epoxides. This increase is higher in epoxy-rich formulations.

The fully cured materials have increasing T_g and decreasing ΔC_p with increasing DG content. This behaviour can be related to the lower mobility of poly(ether) network in comparison with poly(hydroxyamine), caused by the presence of aromatic rings that prevent free bond rotations and with the higher crosslinking density of poly(ether) network. Although JEF in epoxy-amine condensation and DG in epoxy homopolymerization have the same functionality (f=4) the concentration of crosslink points (proportional to the crosslinking density) is higher in poly(ether) network. Theoretical concentration of crosslinking points was calculated as 1.74 and 5.14 mol/kg for DGJEF and DG_BG4, respectively, taking into account the functionality of the monomers, the composition and that all epoxy groups reacted completely.

In Fig. 5, the T_g of the intermediate and final materials as a function of weight compositions are shown for all formulations. As mentioned before, two different trends are seen: a) the T_g of the intermediate materials increase with increasing weight fraction of stage 1, due to the decreasing amount of unreacted epoxy excess at the end of this stage and b) in contrast, the T_g of the final materials increases with decreasing weight fraction of stage 1, due to the higher contribution of the homopolymerization of the excess of epoxy groups. By modifying the stoichiometry of the formulations, thermal characteristics of the intermediate and final materials can be tuned, resulting in properties that range from loosely to tightly crosslinked thermosets. Furthermore, as it will be discussed later, the materials at the end of stage 1 may be above or below the gel point. The former materials are shape-conformable, whereas the latter are suitable as adhesives. Fig. 5 also shows that experimental T_g are in good agreement with those calculated using the Fox equation [43].

3.3. Gelation of epoxy-amine mixtures

The gelation during epoxy-amine reaction was studied by isothermal DSC/TMA combined experiments at 90 °C and the results are summarized in Table 3.

The conversion at gel point, α_{gel}, is strongly affected by composition and monomer functionality, as predicted by the Flory-Stockmayer equation. Amine-rich formulations reach gelation at higher conversions than DG-rich formulations due to the higher functionality of JEF (g=4) compared to DG (f=2 in epoxy-amine condensation). Table 3 shows that the theoretical conversion at gel point α_{gel}^{theor}, and the experimental values α_{gel}^{exp}, show similar trends and have similar values. This result indicates that epoxy-amine polycondensation follows a quasi ideal random step-wise reaction profile. However, the slightly higher α_{gel}^{exp} values can be explained by the intramolecular loop formation causing a delay in gelation, as previously reported for crosslinking of DGEBA with Jeffamine [49,50] and also observed in other epoxy systems [51]. We estimate a critical ratio (r_c) of 3, which is the minimum epoxy/amine ratio to form a gelled and therefore solid-like and shape-conformable intermediate material after stage 1 (see Fig. 5). This ratio was determined using Flory-Stockmayer equation in a similar manner as in a previous work [51]. It can be observed that formulations with $r \geq 4$ (higher than r_c=3) do not reach gelation during DSC/TMA experiments (see Table 3). This is in agreement with the theoretical r_c value of 3. This result suggests that this theoretical r_c can be perfectly used to predict the gelation of the formulations.

Gelation of DG-BG4 formulation was also experimentally determined. Since epoxy homopolymerization is a polyaddition reaction, α_{gel}^{theor} value depends on many factors such as chain transfer reactions, the amount of initiator and its regeneration rate [50,51], which cannot be estimated easily. Despite this, α_{gel}^{exp} attains a similar value to that reported for the homopolymerization of similar epoxy systems.

Gel time decreases with increasing DG content, due to the decrease of α_{gel} and to a certain accelerating effect exerted by the excess of epoxy groups on stage 1. This excess helps amine groups encounter epoxides to react with more easily and leads to a higher initial concentration of catalytic hydroxyl groups coming from the oligomeric structure of DGEBA, in a similar way to what is reported

Table 2
Isothermal reactions heat Δh_1 (Stage 1, 240 min at 90 °C), Δh_2 (Stage 2, 240 min at 180 °C) and Δh_{tot} (obtained as the sum of Δh_1 and Δh_2). T_g and ΔC_p before and after each curing stage in the oven (o, int and ∞ indicate before stage 1, after stage 1 and after stage 2, respectively).

Formulation	T_{go} (°C)	ΔC_{po} (J/gK)	T_{gint} (°C)	ΔC_{pint} (J/gK)	$T_{g\infty}$ (°C)	$\Delta C_{p\infty}$ (J/gK)	Δh_1 (kJ/ee)	Δh_2 (kJ/ee)	Δh_{tot} (kJ/ee)
DGJEF	−47	0.565	49	0.337			99	–	99
DGJEF_0.25_BG4	−38	0.534	36	0.431	71	0.333	77	24	101
DGJEF_0.5_BG4	−32	0,519	23	0.450	89	0.291	49	52	101
DGJEF_0.75_BG4	−21	0.508	7	0.462	98	0.276	29	73	102
DGJEF_0.9_BG4	−16	0,483	−7	0.473	113	0.264	9	88	97
DG_BG4	−14	0.470	–	–	132	0.128	–	95	95

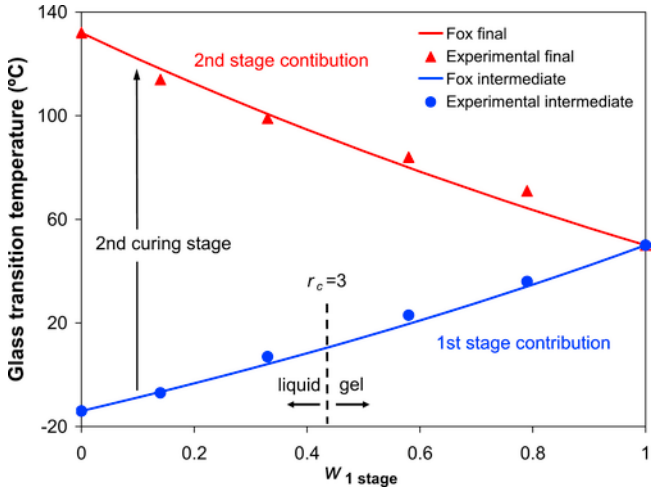

Fig. 5. Intermediate (circles) and final (triangles) experimental glass transition temperatures (T_g) and Fox Equation fits against weight fraction of Stage 1 network. The theoretical minimum Stage 1 wt fraction $W_{1\ stage}$=0.434 (critical ratio of r_c=3) for gelation takes place during stage 1 (shown as a dashed line).

Table 3
Experimental gelation data (α_{gel}^{exp} and t_{gel}) obtained by isothermal FTIR/TMA combined experiments at 90 °C. α_{gel}^{theor} obtained by using Flory-Stockmayer equation.

Formulation	r [a]	α_{gel}^{theor}	α_{gel}^{exp}	t_{gel} (min)
DGJEF	1	0.577	0.650	60.6
DGJEF_0.25_BG4	1.33	0.500	0.560	39.3
DGJEF_0.5_BG4	2	0.408	0.450	31.2
DGJEF_0.75_BG4	4	0.289	Not gel	–
DGJEF_0.9_BG4	10	0.183	Not gel	–
DG_BG4	–	0.200–0.300[b]	0.200	13.4

[a] Ratio between epoxy groups and reactive amine hydrogens.

[b] Range of values experimentally determined for similar epoxy systems [52,53].

for off-stoichiometric thiol-epoxy formulations that are initiated by nucleophilic attack of a tertiary amine [54].

3.4. Storage stability

Storage stability of the intermediate material is a critical feature of latent dual curing systems, especially when these materials are required to be stored for prolonged periods, handled and conformed easily. Higher latency is expected when stage 2 needs to be activated by an external stimulus. For the storage stability test, DSC sample pans were placed in sealed glass tubes which were inserted into thermostatic oil baths at desired temperatures. Storage stability after stage 1 (240 min at 90 °C) was studied by calorimetry. T_g and residual heat were measured after several times of storage at 30 °C, as seen in Fig. 6.

All formulations showed extremely high latency, maintaining their T_g and residual heat constant during storage. This can be explained by the high stability of the BG, previously shown to require temperatures above 120 °C or even higher to be activated. Amine-rich samples have T_g above 30 °C, and are therefore vitrified. Vitrification strongly reduces mobility, helping the material to be stored safely. In conclusion, the higher latency of the intermediate materials is not only controlled by the thermal activation of the latent base with a sufficiently high activation temperature, but also by the vitrification of the formulations with T_g higher than storage temperature.

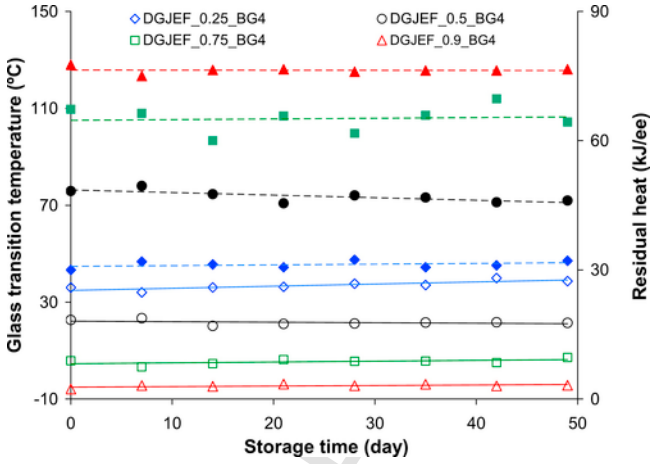

Fig. 6. Intermediate glass transition temperatures (empty symbols and solid regression lines) and residual heat (filled symbols and dashed regression lines) against storage time.

3.5. Dynamomechanical properties of epoxy-amine thermosets

Fig. 7 compares the tan δ and storage moduli of final materials determined by DMA. The relaxation curves are shifted towards higher temperatures with increasing DG content. This indicates an increase in stiffness and degree of crosslinking with increasing DG content, in agreement with calorimetric T_g's shown in Table 2. Different relaxation profiles are observed in the networks formed by step-growth mechanism (epoxy-amine polycondensation, DGJEF formulation) and chain-growth mechanism (anionic epoxy homopolymerization, DG_BG4 formulation), the former showing a narrower relaxation and higher damping capacity (high tanδ peak) and the latter showing a wider relaxation and lower capacity for mechanical energy absorption near its T_g (low tanδ peak), as commonly reported for highly crosslinked thermosets [41].

In general, fully cured materials are highly homogeneous, since DMA curves show singular peaks with no shoulders. The participation of epoxy monomers in both curing stages, ensures the covalent linkage between the two thermosetting networks formed and a higher homogeneity of the material. The final materials are copolymer networks, formed by a combination of poly(hydroxyamine) and poly(ether) networks that are covalently linked to form a single polymer network.

According to the simple rubber elasticity theory, the relaxed modulus determined at $T_{max(tan\ \delta)}$ + 50 °C is inversely proportional to the molecular weight between crosslinking nodes and directly proportional to the crosslinking density [55]. It can also be observed in Fig. 7 that the relaxed modulus increases with increasing DG due to the formation of a more rigid and highly crosslinked structure. As it was previously mentioned, the presence of aromatic rings in DG and the higher concentration of crosslinking points in epoxy-rich formulations are responsible for this behaviour.

Inset of Fig. 7 shows the tan δ curve of intermediate materials that gelled (i.e. have conversions above the gel point conversion) during stage 1. These formulations are DGJEF_0.25_BG4 and DGJEF_0.5_BG4. As it is expected, both formulations show higher damping capacity than fully cured samples due to their low degree of crosslinking and to the flexibilizing effect of the unreacted epoxy excess. Consequently DGJEF_0.25_BG4 has a higher $T_{max(tan\ \delta)}$ and lower tanδ peak in comparison with DGJEF_0.5_BG4 due to a relatively lower epoxy excess. As will be explained later, the temperature

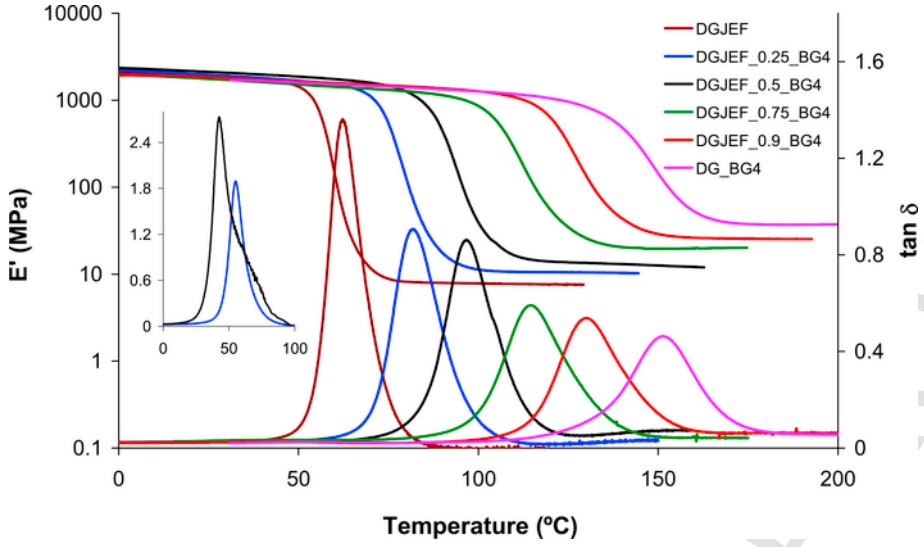

Fig. 7. Storage moduli and tanδ curves as function of temperature of fully cured epoxy-amine formulations. Inset shows tanδ-*T* curves of intermediate materials that gelled during stage 1. The same legend applies to the inset.

ranges where tan δ peaks appeared suggest that gelled intermediate materials are highly shape-conformable at near-ambient temperatures.

3.6. Thermal stability of epoxy-amine thermosets

Fig. 8 shows the thermogravimetric curves for all formulations studied. It can be observed that the degradation took place in two steps except for neat samples DGJEF and DG_BG4 (in Fig. 8b, observe the shoulders in the negative peaks of all non-neat formulations). These degradation steps can be easily assigned to the constituent parts as their temperatures correspond to the degradation temperatures of DGJEF and DG_BG4 samples. The first degradation step, taking place at the temperature range of 300–450 °C, corresponds to the degradation of the poly(hydroxyamine) network, due to the high content of labile C–N bonds and 2-hydroxypropyl units. The second degradation step occurring at the temperature range 400–500 °C can be attributed to the degradation of the poly(ether) structure. The weight loss associated with each degradation step approximately correlates with the weight composition of the dual-curing formulations. This effect is similar to what was reported for dual-curing systems based on the aza-Michael reaction and radical homopolymerization of excess acrylates [17].

The thermal behaviour observed is related fundamentally to the different stabilities of C–N and C–O bonds formed during stage 1 and stage 2, respectively, as previously reported for off-stoichiometric epoxy-amine networks [25], and to the high content of 2-hydroxypropylene groups in the epoxy-amine network. It is also due to the high croslinking density of epoxy homopolymer which constitutes a more thermally stable network. The major weight loss at 300-350 °C is caused by dehydration due to elimination of water molecules from 2-hydroxypropylene groups. This dehydration is concurrent with network breakdown [56].

3.7. Prospective applications

In this section, we explore application possibilities of the prepared materials. First of all, we tested the intermediate material as adhesive bonding. We used DGJEF_0.9_BG4 and DGJEF_0.75_BG4 since they were in liquid form at the intermediate stage. The material was applied onto two glass slides which were clamped together. After performing stage 2 curing, it was observed that the two slides had ad-

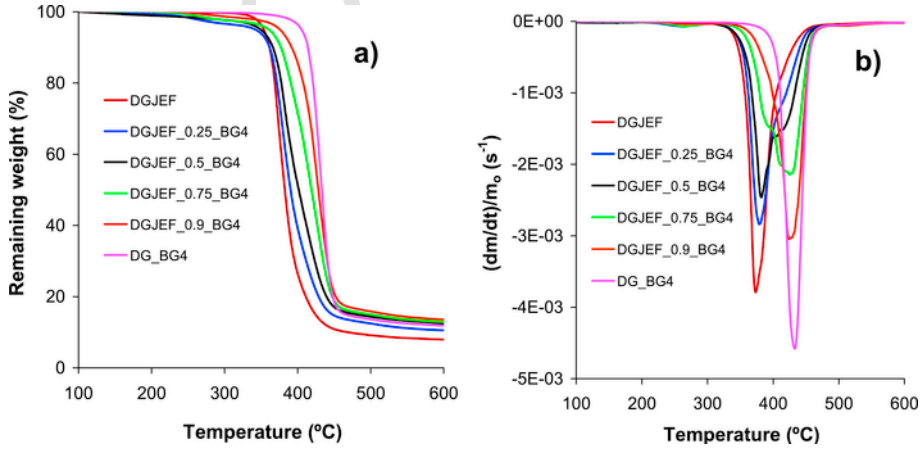

Fig. 8. Remaining weight curves (a) and rate of weight loss (b) against temperature at 10 °C/min in nitrogen atmosphere of fully cured formulations.

hered to each other perfectly and they could not be separated by any hand manipulation.

Secondly, we investigated the conformability of the intermediate materials which had gelled. Fig. 9 illustrates the simple procedure employed. After preparing the formulation DGJEF_0.5_BG4 as described in the experimental section, it was poured into a mould and cured at 90 °C for 240 min to obtain an intermediate prismatic-shaped material with a T_g of 23 °C (see Fig. 9a). Thanks to the deformability of this intermediate material, it was easily rolled onto a glass vial of 24 mm of diameter covered with a layer of Teflon to obtain the bent-shaped surface (permanent shape). Finally, stage 2 was carried out at 180 °C for 240 min and the material (T_g of 89 °C) was peeled off from the vial (see Fig. 9, sequence b-c-d). Objects with other shape and dimensions were also prepared following a similar procedure. The shape-memory characterization was divided into two steps: (1) Programming of the temporary-shape and (2) recovery of the original shape. The programming of the temporary shape was performed between two stainless steel plates at 95 °C (programming temperature) applying sufficient pressure to flatten the sample (see Fig. 9e). Slowly cooled down to room temperature, the material maintained its prismatic-shape. Once the shape was programmed, the recovery of the original bent-shape was facilitated by immersing the sample into a silicon bath at 100 °C. Fig. 9f shows that the recovery of the permanent shape takes place in approximately 31 s. This shape memory effect shown for off-stoichiometric amine-epoxy gels at the intermediate stage can be exploited to prepare shape-memory actuators in the same way as off-stoichiometric thiol-epoxy thermosets [5].

Since the results obtained in shape memory foreshadow interesting applications, the characterization of this behaviour will be carried out in a future project. Due to the similarity of this epoxy-amine system with the off-stoichiometric thiol-epoxy dual-curing system [5,23,51], the behaviour of both systems will be compared in shape memory context.

4. Conclusions

A new family of off-stoichiometric amine-epoxy thermosets with latent reactivity was developed using a dual-curing process. The first stage of curing is a self-limiting epoxy-amine polycondensation at a moderately elevated temperature and the second stage is an anionic epoxy homopolymerization carried out at a higher temperature. The dual-curing process is sequential and the intermediate materials can be safely stored at room temperature for long periods of time. This stability is fundamentally controlled by the thermal activation of the latent base and to a lesser extent by the vitrification of the materials during the first curing stage. Tailoring of the material properties in the intermediate and final curing stages is possible by modifying the amount of epoxy excess in the formulation and therefore the extent of epoxy-amine polycondensation and epoxy homopolymerization reactions. Consequently, it is possible to design intermediate materials which can have conversions above or below the gel point conversion, and fully cured materials which can be loosely or tightly crosslinked. Depending on the composition of the formulations, intermediate materials can be used as adhesives or manipulated to create complex shaped objects with shape memory properties after being fully cured.

Acknowledgments

The authors would like to thank MINECO (Ministerio de Economía, Industria y Competividad) (MAT2017-82849-C2-1-R and MAT2017-82849-C2-2-R) and Generalitat de Catalunya (2017-SGR-77 and Serra Húnter programme) for the financial support.

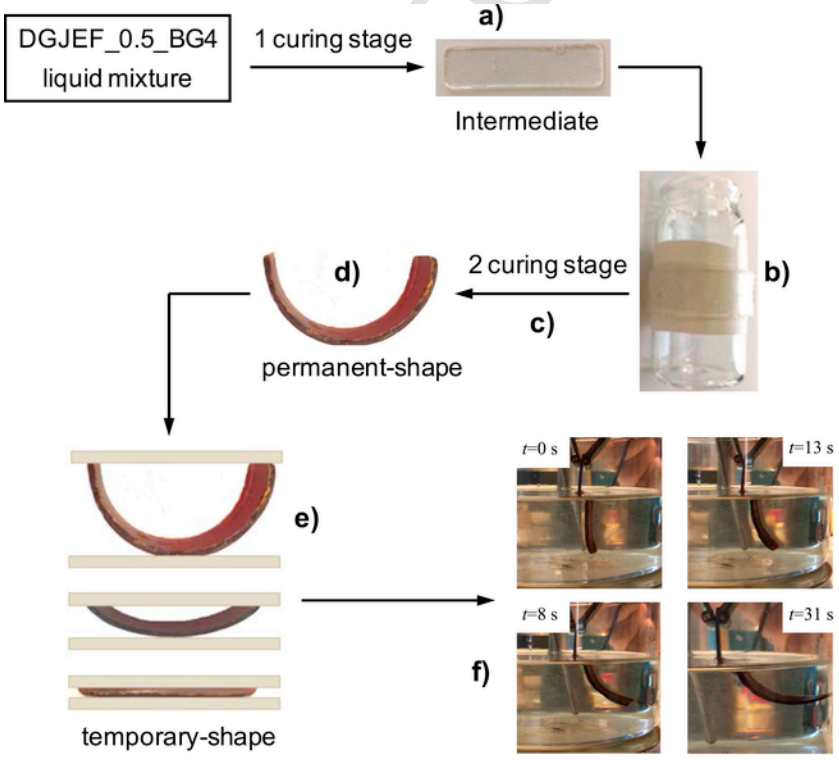

Fig. 9. Illustration of the bent-shaped sample processing, shape-memory programming and recovery process. After Stage 1 curing (a), solid intermediates are rolled onto glass vials (b), stage 2 cured (c) and peeled off (d). Temporary shape was induced slightly above T_g after which the sample was cooled to RT (e). Shape recovery was observed once temperature is increased above T_g (f).

References

[1] X. Ramis, X. Fernández-Francos, S. De La Flor, F. Ferrando, À. Serra, Click-based dual-curing thermosets and their applications, in: Q. Guo (Ed.), Thermosets 2nd Ed. Structure, Properties and Application, Elsevier, 2018, pp. 511–541, https://doi.org/10.1016/B978-0-08-101021-1.00016-2, Ch.16.

[2] O. Konuray, X. Ramis, X. Fernández-Francos, À. Serra, State of the art in dual-curing acrylate systems, Polymers 10 (178) (2018) 1–24, https://doi.org/10.3390/polym10020178.

[3] D.P. Nair, N.B. Cramer, J.C. Gaipa, M.K. McBride, E.M. Matherly, R.R. McLeod, R. Shandas, C.N. Bowman, Two-stage reactive polymer network forming systems, Adv. Funct. Mater. 22 (2012) 1502–1510, https://doi.org/10.1002/adfm.201102742.

[4] S. Chatani, C. Wang, M. Podgórski, C.N. Bowman, Triple shape memory materials incorporating two distinct polymer networks formed by selective thiol–michael addition reactions, Macromolecules 47 (2014) 4949–4954, https://doi.org/10.1021/ma501028a.

[5] A. Belmonte, C. Russo, V. Ambrogi, X. Fernández-Francos, S. De la Flor, Epoxy-based shape-memory actuators obtained via dual-curing of off-stoichiometric thiol–epoxy mixtures, Polymers 9 (113) (2017) 1–19, https://doi.org/10.3390/polym9030113.

[6] A. Belmonte, G.C. Lama, G. Gentile, P. Cerruti, V. Ambrogi, X. Fernández-Francos, S. De la Flor, Thermally-triggered free-standing shape-memory actuators, Eur. Polym. J. 97 (2017) 241–252, https://doi.org/10.1016/j.eurpolymj.2017.10.006.

[7] F. Saharil, F. Forsberg, Y. Liu, P. Bettotti, N. Kumar, F.N. Haraldsson, W.v der-Wijngaart, K.B. Gylfason, Dry adhesive bonding of nanoporous inorganic membranes to microfluidic devices using the OSTE(+) dual-cure polymer, J. Micromech. Microeng. 23 (2013) 025021, https://doi.org/10.1088/0960-1317/23/2/025021.

[8] H. Matsushima, J. Shin, C.N. Bowman, C.E. Hoyle, Thiol-isocyanate-acrylate ternary networks by selective thiol-click chemistry, J. Polym. Sci. Part A Polym. Chem. 48 (2010) 3255–3264, https://doi.org/10.1002/pola.24102.

[9] J. Shin, H. Matsushima, C.M. Comer, C.N. Bowman, C.E. Hoyle, Thiol-isocyanate-ene ternary networks by sequential and simultaneous thiol click reactions, Chem. Mater. 22 (2010) 2616–2625, https://doi.org/10.1021/cm903856n.

[10] V.S. Khire, Y. Yi, N.A. Clark, C.N. Bowman, Formation and surface modification of nanopatterned thiol-ene substrates using step and flash imprint lithography, Adv. Math. 20 (2008) 3308–3313, https://doi.org/10.1002/adma.200800672.

[11] W. Xi, H. Peng, A. Aguirre-Soto, C.J. Kloxin, J.W. Stansbury, C.N. Bowman, Spatial and temporal control of thiol-Michael addition via photocaged superbase in photopatterning and two-stage polymer networks formation, Macromolecules 47 (2014) 6159–6165, https://doi.org/10.1021/ma501366f.

[12] K. Efimenko, J. Finlay, M.E. Callow, J.A. Callow, J. Genzer, Development and testing of hierarchically wrinkled coatings for marine antifouling, ACS Appl. Mater. Interfaces 1 (2009) 1031–1040, https://doi.org/10.1021/am9000562.

[13] C.S. Davis, D. Martina, C. Creton, A. Lindner, A.J. Crosby, Enhanced adhesion of elastic materials to small-scale wrinkles, Langmuir 28 (2012) 14899–14908, https://doi.org/10.1021/la302314z.

[14] S.J. Ma, S.J. Mannino, N.J. Wagner, C.J. Kloxin, Photodirected formation and control of wrinkles on a thiol-ene elastomer, ACS Macro Lett. 2 (2013) 474–477, https://doi.org/10.1021/mz400166e.

[15] H. Peng, D.P. Nair, B.A. Kowalski, W. Xi, T. Gong, C. Wang, M. Cole, N.B. Cramer, X. Xie, R.R. McLeod, C.N. Bowman, High performance graded rainbow holograms via two-stage sequential orthogonal thiol-click chemistry, Macromolecules 47 (2014) 2306–2315, https://doi.org/10.1021/ma500167x.

[16] H. Peng, C. Wang, W. Xi, B.A. Kowalski, T. Gong, X. Xie, W. Wang, D.P. Nair, R.R. McLeod, C.N. Bowman, Facile image patterning via sequential thiol–michael/thiol–Yne click reactions, Chem. Mater. 26 (2014) 6819–6826, https://doi.org/10.1021/cm5034436.

[17] G. Gonzalez, X. Fernandez-Francos, A. Serra, M. Sangermano, X. Ramis, Environmentally-friendly processing of thermosets by two-stage sequential aza-Michael addition and free-radical polymerization of amine-acrylate mixtures, Polym. Chem. 6 (2015) 6987–6997, https://doi.org/10.1039/c5py00906e.

[18] A.O. Konuray, A. Ruiz, J.M. Morancho, J.M. Salla, X. Fernández-Francos, À. Serra, X. Ramis, Sequential dual curing by selective Michael addition and free radical polymerization of acetoacetate-acrylate-methacrylate mixtures, Eur. Polym. J. 98 (2018) 39–46, https://doi.org/10.1016/j.eurpolymj.2017.11.003.

[19] A.O. Konuray, X. Fernández-Francos, À. Serra, X. Ramis, Sequential curing of amine-acrylate-methacrylate mixtures based on selective aza-Michael addition followed by radical photopolymerization, Eur. Polym. J. 84 (2016) 256–267, https://doi.org/10.1016/j.eurpolymj.2016.09.025.

[20] M. Retailleau, A. Ibrahim, C. Croutxé-Barghorn, X. Allonas, C. Ley, D. Le Nouen, One-pot three-step polymerization system using double click Michael addition and radical photopolymerization, ACS Macro Lett. 4 (2015) 1327–1331, https://doi.org/10.1021/acsmacrolett.5b00675.

[21] W. Xi, H. Peng, A. Aguirre-Soto, C.J. Kloxin, J.W. Stansbury, C.N. Bowman, Spatial and temporal control of thiol-Michael addition via photocaged superbase in photopatterning and two-stage polymer networks formation, Macromolecules 47 (2014) 6159–6165, https://doi.org/10.1021/ma501366f.

[22] N. Moszner, V. Rheinberger, Reaction behaviour of monomeric β-ketoesters, 4. Polymer network formation by Michael reaction of multifunctional acetoacetates with multifunctional acrylates, Macromol. Rapid Commun. 16 (1995) 135–138, https://doi.org/10.1002/marc.1995.030160207.

[23] X. Fernández-Francos, A.-O. Konuray, A. Belmonte, S. De la Flor, À. Serra, X. Ramis, Sequential curing of off-stoichiometric thiol–epoxy thermosets with a custom-tailored structure, Polym. Chem. 7 (2016) 2280–2290, https://doi.org/10.1039/C6PY00099A.

[24] A.N. Mauri, C.C. Riccardi, The effect of epoxy excess on the kinetics of an epoxy–anhydride system, J. Appl. Polym. Sci. 85 (2002) 2342–2349, https://doi.org/10.1002/app.10867.

[25] X. Fernandez-Francos, D. Santiago, F. Ferrando, X. Ramis, J.M. Salla, Â. Serra, M. Sangermano, J. Polym. Sci., Part B: Polym. Phys. 50 (2012) 1489–1503, https://doi.org/10.1002/polb.23145.

[26] J.M. Morancho, X. Ramis, X. Fernández-Francos, J.M. Salla, A.O. Konuray, À. Serra, Curing of off-stoichiometric amine-epoxy thermosets, J. Therm. Anal. Calorim. 127 (2018) 645–654, https://doi.org/10.1007/s10973-016-5376-z.

[27] M. Shirai, M. Tsunooka, Photoacid and photobase generator chemistry and applications to polymeric materials, Prog. Polym. Sci. 21 (1996) 1–45, https://doi.org/10.1016/0079-6700(95)00014-3.

[28] A. Gigot, M. Sangermano, L.C. Capozzi, K. Dietliker, In-situ synthesis of organic-inorganic coatings via a photolatent base catalyzed Michael-addition reaction, Polymer 68 (2015) 195–201, https://doi.org/10.1016/j.polymer.2015.05.019.

[29] K. Arimitsu, Y. Takemori, A. Nakajima, A. Oguri, M. Furutani, T. Gunji, Y. Abe, Photobase generators derived from trans-o-coumaric acid for anionic UV curing systems without gas generation, J. Polym. Sci. Part B: Polym. Chem. 53 (2015) 1174–1177, https://doi.org/10.1002/pola.27552.

[30] X. Sun, J.P. Gao, Z.Y. Wang, Bicyclic guanidinium tetraphenylborate: a photobase Generator and A Photocatalyst for living anionic ring-opening polymerization and cross-linking of polymeric materials containing ester and hydroxy groups, J. Am. Chem. Soc. 130 (2008) 8130–8131, https://doi.org/10.1021/ja802816g.

[31] T. Rodima, I. Kaljurand, A. Pihl, V. Mäemets, I. Leito, I.A. Koppel, Acid-base equilibria in nonpolar media. 2.[1] Self-consistent basicity scale in THF solution ranging from 2-methoxypyridine to EtP_1(pyrr) phosphazene, J. Org. Chem. 67 (2002) 1873–1881, https://doi.org/10.1021/jo016185p.

[32] S. Chatani, T. Gong, B.A. Earle, M. Podgorski, C.N. Bowman, Visible-light initiated thiol-Michael addition photopolymerization reactions, ACS Macro Lett. 3 (2014) 315–318, https://doi.org/10.1021/mz500132j.

[33] A.O. Konuray, X. Fernández-Francos, X. Ramis, Latent curing of epoxy-thiol thermosets, Polymer 116 (2017) 191–203, https://doi.org/10.1016/j.polymer.2017.03.064.

[34] Y. Jian, Y. He, Y. Sun, H. Yang, W. Yang, J. Nie, Thiol-epoxy/thiol-acrylate hybrid materials synthesized by photopolymerization, J. Mater. Chem. C 1 (2013) 4481–4489, https://doi.org/10.1039/c3tc30360h.

[35] J. Shin, J. Lee, H.M. Jeong, Properties of polythiourethanes prepared by thiol–isocyanate click reaction, J. Appl. Polym. Sci. 135 (2018) 1–8, https://doi.org/10.1002/APP.46070, 46070.

[36] A.O. Konuray, X. Fernández-Francos, X. Ramis, Curing kinetics and characterization of dual-curable thiol-acrylate-epoxy thermosets with latent reactivity, React. Funct. Polym. 122 (2017) 60–67, https://doi.org/10.1016/j.reactfunctpolym.2017.11.010.

[37] A.O. Konuray, F. Liendo, X. Fernández-Francos, A. Serra, M. Sangermano, X. Ramis, Sequential curing of thiol-acetoacetate-acrylate thermosets by latent Michael addition reactions, Polymer 113 (2017) 193–199, https://doi.org/10.1016/j.polymer.2017.02.072.

[38] W.G. Kim, H. Chun, Cure properties of naphthalene-based epoxy resin systems with hardeners and latent catalysts for semiconductor packaging materials, Mol. Cryst. Liq. Cryst. 579 (2013) 39–49, https://doi.org/10.1080/15421406.2013.805071.

[39] H. Maka, T. Spychaj, R. Pilawka, Epoxy resin/ionic liquid systems: the influence of imidazolium cation size and anion type on reactivity and thermo-

mechanical properties, Ind. Eng. Chem. Res. 51 (2012) 5197–5206, https://doi.org/10.1021/ie202321j.
[40] R. Thomas, C. Sinturel, J. Pionteck, H. Puliyalil, S. Thomas, In-situ cure and cure kinetic analysis of a liquid rubber modified epoxy resin, Ind. Eng. Chem. Res. 51 (2012) https://doi.org/10.1021/ie2029927, 12178–1219.
[41] J.P. Pascault, H. Sautereau, J. Verdu, R.J.J. Williams, Thermosetting Polymers, Marcel Dekker, New York, 2002.
[42] J.P. Pascault, R.J.J. Williams, Overview of thermosets: present and future, in: Q. Guo (Ed.), Thermosets 2nd Ed. Structure, Properties and Application, Elsevier, 2018, pp. 3–34, https://doi.org/10.1016/B978-0-08-101021-1.00001-0, Ch.11.
[43] T.G. Fox, Influence of diluent and of copolymer composition on the glass temperature of a polymer system, Bull. Am. Phys. Soc. 1 (1956) 123.
[44] K.J. Ivin, in: J. Brandrup, E.H. Immergut (Eds.), Polymer Handbook, Wiley, New York, 1975.
[45] S.K. Ooi, W.D. Cook, G.P. Simon, C.H. Such, DSC studies of the curing mechanisms and kinetics of DGEBA using imidazole curing agents, Polymer 41 (2000) 3639–3649, https://doi.org/10.1016/S0032-3861(99)00600-X.
[46] D. Santiago, X. Fernàndez-Francos, X. Ramis, J.M. Salla, M. Sangermano, Comparative curing kinetics and thermal–mechanical properties of DGEBA thermosets cured with a hyperbranched poly(ethyleneimine) and an aliphatic triamine, Thermochim. Acta 529 (2011) 9–21, https://doi.org/10.1016/j.tca.2011.08.016.
[47] X. Fernandez-Francos, W.D. Cook, A. Serra, X. Ramis, G.G. Liang, J.M. Salla, Crosslinking of mixtures of DGEBA with 1,6-dioxaspiro[4,4]nonan-2,7-dione initiated by tertiary amines. Part IV. Effect of hydroxyl groups on initiation and curing kinetics, Polymer 51 (2010) 26–34, https://doi.org/10.1016/j.polymer.2009.11.013.
[48] B.A. Rozenberg, Kinetics, thermodynamics and mechanism of reactions of epoxy oligomers with amines, Adv. Polym. Sci. 75 (1986) 113–165.
[49] L. Matejka, Amine cured epoxide Networks: formation, structure, and properties, Macromolecules 33 (2000) 3611–3619, https://doi.org/10.1021/ma991831w.
[50] Y. Tanaka, J.L. Stanford, R. Stepto, Interpretation of gel points of an epoxyamine system including ring formation and unequal reactivity: measurements of gel points and analyses on ring structures, Macromolecules 45 (2012) 7197–7205, https://doi.org/10.1021/ma300984u.
[51] A. Belmonte, X. Fernández-Francos, À. Serra, S. De la Flor, Phenomenological characterization of sequential dual-curing of off-stoichiometric “thiol-epoxy” systems: towards applicability, Mater. Des. 113 (2017) 116–127, https://doi.org/10.1016/j.matdes.2016.10.009.
[52] X. Fernandez-Francos, W.D. Cook, A. Serra, X. Ramis, G.G. Liang, J.M. Salla, Crosslinking of mixtures of DGEBA with 1,6-dioxaspiro[4,4]nonan-2,7-dione initiated by tertiary amines. Part III. Effect of hydroxyl groups on network formation, Polym. Int. 58 (2009) 1401–1410, https://doi.org/10.1002/pi.267.
[53] L. Matějka, P. Chabanne, L. Tighzert, J.P. Pascault, Cationic polymerization of diglycidyl ether of bisphenol A, J. Polym. Sci., Part A: Polym. Chem. 32 (1994) 1447–1458, https://doi.org/10.1002/pola.1994.080320806.
[54] A.O. Konuray, X. Fernandez-Francos, X. Ramis, Analysis of the reaction mechanism of the thiol-epoxy addition initiated by nucleophilic tertiary amines, Polym. Chem. 8 (2017) 5934–5947, https://doi.org/10.1039/c7py01263b.
[55] L.E. Nielsen, J. Macromol. Sci. Rev. Macromol. Chem. 3 (1969) 69–103.
[56] H.W. Moeller, Progress in Polymer Degradation and Stability Research, Nova Science Publishers, Inc, New Cork, 2008.